Estimating the Arterial Input Function Using Two Reference Tissues in Dynamic Contrast-Enhanced MRI Studies: Fundamental Concepts and Simulations

Cheng Yang,[1] Gregory S. Karczmar,[2,3] Milica Medved[2] and Walter M. Stadler[1,3*]

In dynamic contrast-enhanced MRI (DCE-MRI) studies, an accurate knowledge of the arterial contrast agent concentration as a function of time is crucial for the estimation of kinetic parameters. In this work, a novel method for estimating the arterial input function (AIF) based on the contrast agent concentration-vs.-time curves in two different reference tissues is described. It is assumed that the AIFs of the two tissues have the same shape, and that simple models with two or more compartments, and unknown kinetic parameters, can describe their tracer concentration-vs.-time curves. Based on the principle of self-consistency, one can relate the two tracer concentration-vs.-time curves to estimate their common underlining AIF, together with the kinetic parameters of the two tissues. In practice, the measured concentration-vs.-time curves have noise, and the AIFs of the two tissues are not exactly the same due to different dispersion effects. These factors will produce errors in the AIF estimate. Simulation studies show that despite the two error sources, the double-reference-tissue method provides reliable estimates of the AIF. Magn Reson Med 52: 1110–1117, 2004. © 2004 Wiley-Liss, Inc.

Key words: dynamic MRI; contrast agent; arterial input function; pharmacokinetic model; Gd-DTPA

In clinical and experimental dynamic contrast-enhanced MRI (DCE-MRI) studies, a low-molecular-weight, extracellular contrast agent (such as Gd-DTPA) is commonly injected, and its concentration-vs.-time curve in vivo is measured with the use of T_1-weighted images. A number of kinetic models have been proposed to characterize the concentration-vs.-time curves and infer the tissue's physiologic properties. The quantities that can be estimated from the kinetic models are often referred to as kinetic parameters, and some of them reflect local physiology. The most widely used kinetic model is the two-compartment model (1–3), which attributes the concentration change of the contrast agent to its transfer between two compartments: the blood plasma and the tissue extravascular extracellular space (EES). Given the tracer concentration in the arterial blood plasma as a function of time, which is often referred to as the contrast agent arterial input function (AIF), through curve fitting we can obtain the transfer constant of the contrast agent (K^{trans}) and the fractional EES volume (ν_e), which respectively reflect the vascular permeability and the leakage space of the tissue. These two kinetic parameters (especially K^{trans}) are now frequently used as surrogate hemodynamic markers to assess drugs that target tumor vasculature (4).

In order to extract meaningful kinetic parameters, most kinetic models, including the two-compartment model, require a precise measurement of contrast agent concentration, and an accurate estimation of the AIF. To date, the AIF has been extremely difficult to estimate or measure in clinical DCE-MRI studies with low-molecular-weight contrast agents. The AIF thus becomes a major source of error in estimates of K^{trans} and other kinetic parameters.

Four methods have been used to estimate the AIF. The most common approach is to use a fixed biexponential AIF, as proposed by Tofts and Kermode (2). This is a robust approach; however, the biexponential function cannot describe the first pass of the contrast media bolus. The use of this biexponential AIF obtained from low-time-resolution experimental data can cause significant error in the estimate of K^{trans} when images are collected with a high time resolution (5). In addition, the variation between individuals in measured AIFs can be as large as 4.5-fold, which would make a mean parameter AIF model highly unreliable (6). The second method is to measure the AIF in a major artery using standard DCE-MRI techniques. Recent studies have shown that under some conditions, the AIF determined in this manner is in good agreement with the AIF determined from direct blood sampling (7). However, direct measurement of the arterial blood concentration of contrast agent by MRI is subject to errors due to T_2^* effects, partial volume effects, low signal-to-noise ratio (SNR) when smaller arteries must be sampled, and errors due to the rapid flow of blood in the artery. In addition, the AIF measured from a major artery can be substantially different from the local AIF in the tissue of interest due to delay and dispersion effects. Simulations suggest that errors as large as 70% of the actual value can be introduced by using the AIF in a major artery to determine kinetic parameters for a specific tissue (8). Finally, for many MRI scans, a major artery may not be in the field of view (FOV).

The third method for estimating the AIF assumes that it can be described by a family of functions with adjustable parameters, but that the kinetic parameters of the tissue are unknown. A best fit of the tissue tracer concentration-vs.-time curve is then claimed to give the best estimates of both the AIF and the kinetic parameters associated with the tissue. For ease of reference, we will refer to this latter method as the curve-fitting method. In the first published application of this method (9), a monoexponential function was used to characterize the shape of the AIF. This

[1]Department of Medicine, University of Chicago, Chicago, Illinois.
[2]Department of Radiology, University of Chicago, Chicago, Illinois.
[3]Cancer Research Center, University of Chicago, Chicago, Illinois.
Grant sponsor: Cancer Center; Grant number: 5 P30 CA14599-29.
*Correspondence to: Walter M. Stadler, M.D., Associate Professor, Department of Medicine, Section of Hematology/Oncology, 5841 S. Maryland, MC2115, Chicago, IL 60637. E-mail: wstadler@medicine.bsd.uchicago.edu
Received 29 December 2003; revised 6 May 2004; accepted 8 June 2004.
DOI 10.1002/mrm.20243
Published online in Wiley InterScience (www.interscience.wiley.com).

assumption potentially introduces significant errors due to the oversimplification of the AIF shape. On the other hand, more complicated AIF models, such as the sum of three Gamma-variate functions (10), are difficult to apply. When the data are noisy and the function used to model the AIF has too many parameters, it becomes difficult to dissociate the AIF parameters from the local kinetic parameters during curve fitting. Thus the results obtained for the AIF and the physiologic parameters have significant errors.

The fourth method is called the reference-tissue approach. It uses a normal reference tissue, which in previous work (11) was assumed to be a two-compartment tissue, to determine the AIF. This approach assumes that values of kinetic parameters of normal tissue do not vary greatly. Literature values for K^{trans} and v_e are used in the two-compartment model for the reference tissue. The contrast agent concentration-vs.-time curve in the reference tissue is measured experimentally. In this case, the only unknown variable is the blood plasma concentration of contrast agent as a function of time, i.e., the AIF. The AIF is inversely derived from the measured concentration-vs.-time curve in the reference tissue. This works well in practice because the two-compartment model provides a good fit to data obtained from normal reference tissues, particularly those with high blood flow. This approach is able to successfully characterize the shape of the AIF, including the first-pass portion (11), and may better reflect the local AIF for the region of interest (ROI) than the AIF measured from a remote major artery. It provides high SNR when a large volume of tissue with rapid blood flow can be used as a reference, and it avoids errors due to partial volume effects that can occur when the AIF is measured directly in arteries. However, the values of the kinetic parameters can vary considerably between different subjects, or even between different scans of the same subject. This may be especially true for parameters that depend on blood flow and capillary permeability, such as K^{trans} (3). Thus, the use of fixed values from the literature is likely to cause significant errors in the estimate of AIF.

Finally, the traditional reference-tissue approach is not self-consistent. For purposes of illustration, suppose there are two reference tissues (e.g., spleen and muscle) within one scan, and that their true AIFs are the same. With each reference tissue we can obtain an estimate of the AIF using the literature values for its kinetic parameters. Because the literature values of the kinetic parameters generally differ from the true values in each particular scan, the two AIFs estimated independently from the two reference tissues may be both different from the true AIF and different from each other, which clearly contradicts our hypothesis that the AIFs of the two tissues are the same.

The lack of self-consistency in the traditional reference-tissue approach is primarily due to the discrepancy between the literature values and the true values of the kinetic parameters. Here we illustrate that by amending the inconsistency between the two estimated AIFs, one can find both the true values of the kinetic parameters *and* the correct estimate of the AIF using two reference tissues (see the Double-Reference-Tissue Method section). We also use simulations to show that the double-reference-tissue method has the potential to be highly accurate despite the use of minimal assumptions and noisy data (see Simulations section).

MATERIALS AND METHODS

Double-Reference-Tissue Method

General Theory

Following the standard notation proposed in Ref. 3, we use $C_p(t)$ and $C_t(t)$ to denote the AIF and the tracer concentration in tissue, respectively, as a function of time. A kinetic model relates $C_t(t)$ and $C_p(t)$ through the kinetic parameters, which we can symbolize as

$$C_t(t) = f(C_p(t),\Omega), \quad [1]$$

where f is a model-dependent function, and Ω represents all of the kinetic parameters. Given the kinetic parameters, we can inversely determine the AIF from $C_t(t)$:

$$C_p(t) = g(C_t(t),\Omega), \quad [2]$$

where $g = f^{-1}$ is the inverse function of f. Equation [2] is the "reference-tissue approach" for obtaining the AIF.

When there are two reference tissues available in the MRI FOV, we propose the use of the double-reference-tissue method to determine the AIF using the two tracer concentration-vs.-time curves. The method is based on the following two assumptions:

1. The AIFs of the two reference tissues have the same shape, but there can be differences in the arrival time of the contrast media bolus.

2. For each reference tissue, we know a priori what kind of kinetic model can adequately explain the concentration-vs.-time curve.

We use superscript A and B to denote the two reference tissues, and l denotes the difference in bolus arrival times between tissue A and tissue B. A positive value means that the bolus arrives in tissue B later than in tissue A. The assumption that the AIFs of the two reference tissues share the same shape enables us to establish a relation between them:

$$g^A(C_t^A(t-l),\Omega^A) = C_p^A(t-l) = C_p^B(t) = g^B(C_t^B(t),\Omega^B). \quad [3]$$

Since we know the appropriate kinetic model for each reference tissue (i.e., the exact form of g^A and g^B), we can use Eq. [3] to estimate the kinetic parameters Ω^A and Ω^B, and hence the AIF of the two tissues. An equivalent equation to Eq. [3] is

$$C_t^B(t) = f^B(C_p^B(t),\Omega^B) = f^B(g^A(C_t^A(t-l),\Omega^A),\Omega^B), \quad [4]$$

which shows that we can estimate the kinetic parameters by fitting the $C_t(t)$ of one reference tissue using information from the other reference tissue. The logic behind this fitting procedure can be explained as follows: If the parameters assumed for reference tissue A are not correct, the AIF obtained deviates from the true underlying AIF so that we cannot get a good fit of the concentration-vs.-time curve

in tissue B. Under the assumptions that the AIF in the two tissues has the same shape, and the kinetic models of the two tissues are known, a correct estimate of the AIF, and thus a best fit of the concentration-vs.-time curve in tissue B, can only be obtained when the parameters assumed for reference tissue A are accurate.

The double-reference-tissue method can be considered as an extension of both the curve-fitting method and the reference-tissue approach. Equation [4] demonstrates that it is closely related to the curve-fitting method, since both methods use curve-fitting to derive the kinetic parameters and the AIF. However, the double-reference-tissue method does not have the difficulty faced by the traditional curve-fitting method in choosing a family of functions to describe the AIF. As shown by Eq. [4], the double-reference-tissue method chooses these functions as $g^A(C_t^A(t - l),\Omega^A)$ inspired by the reference-tissue approach. This choice of functions makes it possible to adequately describe the shape of AIF with a very limited number of parameters. In the example below, we show that, unlike the traditional reference-tissue approach, the double-reference-tissue method can find the true values for most of the kinetic parameters through curve fitting, so that the error due to the disagreement between the literature and actual values can be minimized. As in the traditional reference-tissue approach, the literature values for kinetic parameters provide initial values for their fitting, and can be used to avoid physiologically unrealistic solutions.

Applications to Two-Compartment Reference Tissues

As an example, we will discuss the case in which both reference tissues A and B are well approximated by the two-compartment model. In the two-compartment model, the rate constant K_{ep} is defined as

$$K_{ep} = K^{trans}/v_e, \quad [5]$$

which represents the rate constant of contrast agent backflux from the EES to the blood plasma. Instead of K^{trans} and v_e, we can equivalently choose K_{ep} and v_e as the kinetic parameters. When the intravascular contribution to the measured tracer concentration is ignored, Eqs. [1] and [2] have simple expressions in the two-compartment model:

$$C_t(t) = v_e K_{ep} \int_0^t C_p(\tau)\, \exp[-K_{ep}(t-\tau)]d\tau, \quad [6]$$

$$C_p(t) = \frac{1}{v_e}\left[C_t(t) + \frac{1}{K_{ep}}\frac{dC_t(t)}{dt}\right]. \quad [7]$$

Our eventual goal is to use Eq. [7] to calculate $C_p(t)$ based on the reference-tissue approach. $C_t(t)$ and $dC_t(t)/dt$ can be estimated from the measured concentration-vs.-time curve, which always has noise, but we need the best possible values for v_e and K_{ep}. To obtain these values, we combine data from the two different reference tissues. With the use of $C_t'(t)$ to denote $dC_t(t)/dt$, Eq. [4] becomes

$$C_t^B(t) = \frac{v_e^B}{v_e^A}K_{ep}^B \int_0^t \left[C_t^A(\tau - l) + \frac{1}{K_{ep}^A}C_t'^A(\tau - l)\right] \times \exp[-K_{ep}^B(t-\tau)]d\tau = \frac{v_e^B}{v_e^A}K_{ep}^B\left[\frac{1}{K_{ep}^A}C_t^A(t-l) + \left(1 - \frac{K_{ep}^B}{K_{ep}^A}\right)\int_0^t C_t^A(\tau - l)\exp[-K_{ep}^B(t-\tau)]d\tau\right], \quad [8]$$

where the second equality comes from integration by parts. Equation [8] is used to fit the kinetic parameters of the two reference tissues. Finally, the fitted parameters are plugged into Eq. [7] to estimate the AIF of the reference tissues.

In the double-reference-tissue method, the number of kinetic parameters that can be estimated is one less than the total number. For example, Eq. [8] shows that the values of v_e^A and v_e^B cannot be determined; only their ratio can be estimated. This means that the double-reference tissue alone cannot estimate the amplitude of the AIF according to Eq. [7]. To fix the amplitude of the AIF and obtain all of the kinetic parameters, we can use the literature value of the v_e from one normal reference tissue with small variability, such as liver (12). The other kinetic parameter, K^{trans}, can then be fitted, since it depends on more volatile physiological factors (such as blood flow and capillary permeability), and thus varies more dramatically (3). An alternative way to fix the amplitude of the AIF is to make one or two measurements of tracer concentration in blood during the washout phase. To accomplish this experimentally, one could temporarily change the acquisition parameters to image the heart chamber, the aorta, or some other large artery. This measurement of contrast agent concentration in blood can be interleaved with the primary protocol, which typically focuses on a tumor or tumors. The arterial blood would then serve as an additional reference tissue, but would only be imaged for a few seconds during the washout phase.

When K_{ep}^A is equal to K_{ep}^B, both will disappear in Eq. [8], so we cannot estimate them in this degenerate case. Similarly, when K_{ep}^A is close to K_{ep}^B, the errors in their estimates will be large. To avoid large errors caused by near degeneracy, two reference tissues with very different rate constants (e.g., spleen and nearby skeletal muscle, or liver and muscle) should be chosen.

The measured tracer concentration $\tilde{C}_t(t)$ has noise and only has values at discrete time points t_i, $i = 1,\ldots,n$. However, to perform curve fitting using Eq. [8], for reference tissue A we need a smooth estimate of the true concentration $C_t(t)$ and its first derivative $dC_t(t)/dt$ at any time point during the scan. For this purpose, we assume the following statistical model to describe the noise in the clinical data:

$$\tilde{C}_t(t) = C_t(t) + \sigma(t)\varepsilon, \quad [9]$$

where $C_t(t)$ is the true tracer concentration, $\sigma(t)$ is the standard deviation (SD) of the noise (i.e., the root-mean-square (RMS) noise level at time t), and ε is an uncorre-

lated standard Gaussian random variable. With the noise model (Eq. [9]), the estimation of $C_t(t)$ and its first derivative $dC_t(t)/dt$ can be accomplished with the use of several nonparametric curve-smoothing methods, such as the local polynomial fitting (13) and spline-smoothing (14) methods. When the two reference tissues include one high-blood-flow tissue and one low-blood-flow tissue, the high-blood-flow tissue will be chosen as tissue A, since its measured concentration-vs.-time curve usually has better SNR in the early stage of the contrast agent uptake. As a result, the errors in the estimates of $C_t^A(t)$ and $dC_t^A(t)/dt$ are smaller. For similar reasons, the use of the high-blood-flow tissue (tissue A) is also recommended for reconstructing the AIF using Eq. [7].

When deriving the AIF, the tracer concentration-vs.-time curve from an ROI in the reference tissues, rather than in a single pixel, should be used in order to increase the SNR of the data. The criterion for choosing the ROI is that pixels within the ROI should have very homogenous kinetic properties, which is not difficult to achieve in a normal tissue. After the AIF is determined, it can be used to estimate the kinetic parameters in a tissue of interest—either in an ROI or on a pixel-by-pixel basis.

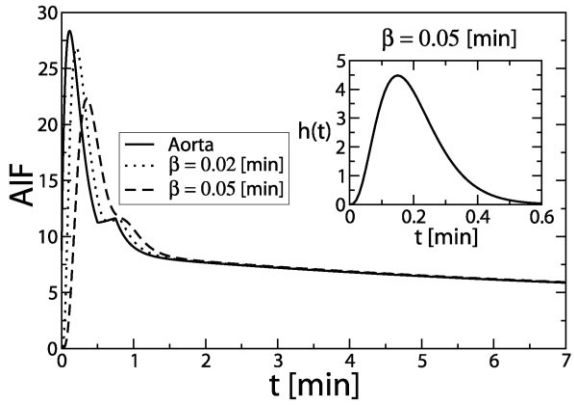

FIG. 1. The effect of dispersion on the shape of simulated AIFs in the reference tissues. The transport function $h(t)$ used in the simulations is a 4th-order Gamma-variate function with scale β. Insert: The shape of $h(t)$ when β = 0.05 [min] and t_o = 0.0 [min]. Solid line: The shape of the AIF in the aorta used in the simulations. Dotted line and dashed lines show the simulated AIFs in the reference tissues when β = 0.02 [min] and β = 0.05 [min], respectively. The larger the β, the larger is the dispersion, and the wider and lower is the first-pass peak.

Simulations

Goals

In real clinical data sets, the assumption that the two reference tissues have AIFs of the same shape may be invalid. For example, the AIFs in the spleen and the nearby spine muscle are very likely not the same, because they undergo different types of dispersion as they travel from the aorta to different capillary beds. Real clinical data also have noise. In this section, we use Monte Carlo simulations (15) to examine the random and systematic errors caused by these two factors. In the following simulations, a two-compartment model for both reference tissues is assumed.

Preparation of the Simulated AIFs

In the simulations, we prepared the AIFs in the two reference tissues by mimicking the dispersion of the AIF in a major artery as it travels to the capillary beds of the reference tissues. The AIF in a reference tissue is mathematically expressed as a convolution:

$$C_p(t) = C_p^{\text{Aorta}}(t) \otimes h(t), \qquad [10]$$

where we use $C_p^{\text{Aorta}}(t)$ to denote the shape of the AIF in the aorta, and $h(t)$ is called the transport function or indicator dilution curve (8). Many mathematical expressions, such as the Gamma-variate function (16,17), the log normal function (18), and the lagged normal density curve (19), have been suggested theoretically or empirically to describe the experimentally measured transport function.

We chose a Gamma-variate function as the transport function in our simulation for simplicity of calculation:

$$h(t) = \frac{1}{\Gamma(\alpha)\beta^{\alpha}}(t - t_o)^{\alpha-1}e^{-(t-t_o)/\beta}, \qquad [11]$$

where t_o is the bolus arrival time, and Γ denotes the complete Gamma function. Since many studies have found that transport functions have fairly similar shapes, except for a different amount of spread (20), we assume that different tissues have the same α equal to 4, but different scales β and bolus arrival time. The assumed transport function $h(t)$ with α = 4 resembles the transport functions seen in many experiments (see Fig. 1 insert for an example) (17–20). In our simulations we also assume the following $C_p^{\text{Aorta}}(t)$ (shown in Fig. 1):

$$C_p^{\text{Aorta}}(t) = 3.99e^{-t/0.144} + 4.78e^{-t/0.0111} + 240(e^{-t/0.125} - e^{-t/0.1}) + 4[(1 - e^{-5(t-0.5)})I(t - 0.5) - (1 - e^{-5(t-0.75)})I(t - 0.75)], \qquad [12]$$

where $I(t)$ represents the unit step function, equal to 0 for $t < 0$ and 1 for $t \geq 0$. Once again, the simple expression in Eq. [12] produces a shape that resembles the AIF measured in a major artery following a bolus injection of contrast agents (7,21,22). The first two terms in Eq. [12] comprise exactly the biexponential function in Ref. 2. We add two more terms to describe the first and second passes observed in experiments so that the simulated data better resemble clinical data. Given the choices of $h(t)$ and $C_p^{\text{Aorta}}(t)$ above, we use Eq. [10] to calculate $C_p(t)$ in the reference tissues. Figure 1 shows that the shape of $C_p(t)$ is highly distinct for different values of β. With larger values of β, the dispersion is larger, and the first-pass peak is wider and lower. Thus, when we select different values of β for the two reference tissues ($\beta^A \neq \beta^B$), their AIFs have different shapes. In clinical data, the bolus arrival time t_o depends on the contrast agent injection time, but often differs in different tissues. One can simulate the effect of t_o by simply shifting the AIF in the reference tissue. In our simulations, the bolus arrival time of tissue A, t_o^A, is set to

Table 1
The Means and Confidence Intervals (C. I.) of the Fitted Parameters When $\beta^A = \beta^B$ With Several Different Sets of Simulation Parameters*

$\beta^A = \beta^B$ (min)	σ^A	σ^B	$(K^A_{ep})^{-1}$ (min) Mean (95% C. I.)	K^B_{ep} (min^{-1}) Mean (95% C. I.)	v^B_e/v^A_e Mean (95% C. I.)	l (min) Mean (95% C. I.)
0.02	0.10	0.050	0.401 (0.346, 0.459)	0.500 (0.469, 0.530)	0.5001 (0.4924, 0.5090)	0.141 (0.117, 0.162)
0.02	0.05	0.025	0.400 (0.374, 0.428)	0.500 (0.485, 0.515)	0.5000 (0.4961, 0.5042)	0.140 (0.129, 0.152)
0.05	0.10	0.050	0.400 (0.341, 0.460)	0.500 (0.468, 0.532)	0.5001 (0.4918, 0.5087)	0.140 (0.113, 0.167)
0.05	0.05	0.025	0.401 (0.369, 0.430)	0.500 (0.485, 0.515)	0.5001 (0.4958, 0.5042)	0.141 (0.126, 0.154)

*The "true" values of the parameters, i.e., the values selected for the simulations are: $(K^A_{ep})^{-1} = 0.4$ (min), $K^B_{ep} = 0.5$ (min^{-1}), $v^B_e/v^A_e = 0.5$, and $l = 0.14$ (min).

the clinically reasonable value $t = 0.7$ min, and the bolus arrival time in tissue B is $t^B_o = t^A_o + l$, with $-0.28 \le l \le 0.28$ [min].

Kinetic Parameters

In the clinical application of the double-reference-tissue method, we typically choose one high-blood-flow tissue (e.g., spleen or liver) as reference tissue A, and one low-blood-flow tissue (e.g., skeletal muscle) as reference tissue B. Accordingly, in our simulations we select the kinetic parameters of the two tissues as ($K^A_{ep} = 2.5$ [min^{-1}], $v^A_e = 0.28$) and ($K^B_{ep} = 0.5$ [min^{-1}], $v^B_e = 0.14$), which are similar to the kinetic parameters of spleen and muscle for Gd-DTPA, respectively (23,24).

Simulation Procedures

In the first step of the simulations, given the AIF and kinetic parameters, we use Eq. [6] to calculate the "true" concentration-vs.-time curves $C^A_t(t)$ and $C^B_t(t)$ (the word "true" is in quotation marks because it refers to simulations). In step 2, random Gaussian noise is added to produce simulated curves $\tilde{C}^A_t(t)$ and $\tilde{C}^B_t(t)$ according to the noise model in Eq. [9], assuming that the noise level $\sigma(t)$ is constant. The simulated concentration-vs.-time curves have 400 equally spaced time points during a time period of 7 min. The third step is to estimate the kinetic parameters by a nonlinear least-square fitting of $\tilde{C}^B_t(t)$ based on Eq. [8]. First, a local polynomial regression is used to smooth $\tilde{C}^A_t(t)$ to obtain the estimates of $C^A_t(t)$ and $dC^A_t(t)/dt$, and then the four parameters K^A_{ep}, K^B_{ep}, v^B_e/v^A_e, and l are fitted by means of the Levenberg-Marquardt algorithm (25). We use a 4th-order local polynomial regression to optimize the estimation of $dC^A_t(t)/dt$, and a variable bandwidth selection scheme to capture the complicated shapes of the curves (13). All of the numerical integrations needed to fit $\tilde{C}^B_t(t)$ are performed according to Simpson's rule (25). For each set of simulation parameters, steps 2 and 3 are repeated 1000 times using the same noise level. With such a large number of repetitions, the 95% confidence interval (C.I.) of each fitted parameter can be simply constructed by the 2.5% and 97.5% quintiles of the 1000 fitted values. Two sets of noise levels are used in our simulations: ($\sigma^A(t) = 0.10$, $\sigma^B(t) = 0.05$) and ($\sigma^A(t) = 0.05$, $\sigma^B(t) = 0.025$). The corresponding SNRs for concentration are about 20 and 40, respectively, at $t = 7.0$ min. In terms of time resolution and SNR, the simulated data are comparable to DCE-MRI clinical data from a typical ROI scanned with TE = 1.7 ms, TR = 8 ms, and flip angle = 60° at 1.5 Tesla (26).

RESULTS

First, we set $\beta^A = \beta^B$ to determine whether the double-reference-tissue method works in principle when the AIFs of the two reference tissues have the same shape. The various AIFs shown in Fig. 1 were used in our simulation. Table 1 summarizes the statistics of the four fitted parameters with several different sets of simulation parameters. It shows that the means of the fitted parameters are always very close to the "true" values (i.e., the values selected for the simulations). Student's t-tests confirmed that the estimates were unbiased (data not shown). The 95% C.I. has a small half-width. For example, at the noise level ($\sigma^A(t) = 0.10$, $\sigma^B(t) = 0.05$), the half-width of the 95% C.I. of the fitted $(K^A_{ep})^{-1}$ is approximately 15% of its "true" value of 0.4. Instead of the rate constant K^A_{ep} itself, we tabulated it as inverse because the resulting error in the estimated AIF is proportional to the error in the fitted $(K^A_{ep})^{-1}$ according to Eq. [7]. When the noise level is decreased by half, the 95% C.I. width reduces by approximately half as well. In Table 1 we report only the case of $l = 0.14$ [min]. The results are similar for other values of l.

To illustrate the performance of the double-reference-tissue method, we chose one data set out of the total of 1000 simulated ones created at $\beta^A = \beta^B = 0.02$ [min], noise level ($\sigma^A(t) = 0.10$, $\sigma^B(t) = 0.05$), and $l = 0.14$ [min]. We used the sum of squared errors (SSE) to measure the performance of the fit. SSE is defined as

$$SSE = \sum_{i=1}^{n} [\hat{C}^B_t(t_i) - C^B_t(t_i)]^2, \qquad [13]$$

where $\hat{C}^B_t(t_i)$ is the concentration in tissue B estimated by the double-reference-tissue method. Out of the 1000 simulated data sets used, we report on the one with median SSE, and thus median performance of fit (illustrated in Fig. 2). Figure 2d shows the histogram of the total of 1000 fitted $(K^A_{ep})^{-1}$ determined from the 1000 simulated data sets, together with the fitted $(K^A_{ep})^{-1}$ of the data set with median SSE. With a value equal to 0.381 [min], this fitted $(K^A_{ep})^{-1}$ is the 26% quantile; it is closer to the "true" value (0.4) than 52% of the 1000 fitted $(K^A_{ep})^{-1}$. Thus, the current example with median SSE shows an approximately median performance in terms of the difference between the fitted $(K^A_{ep})^{-1}$

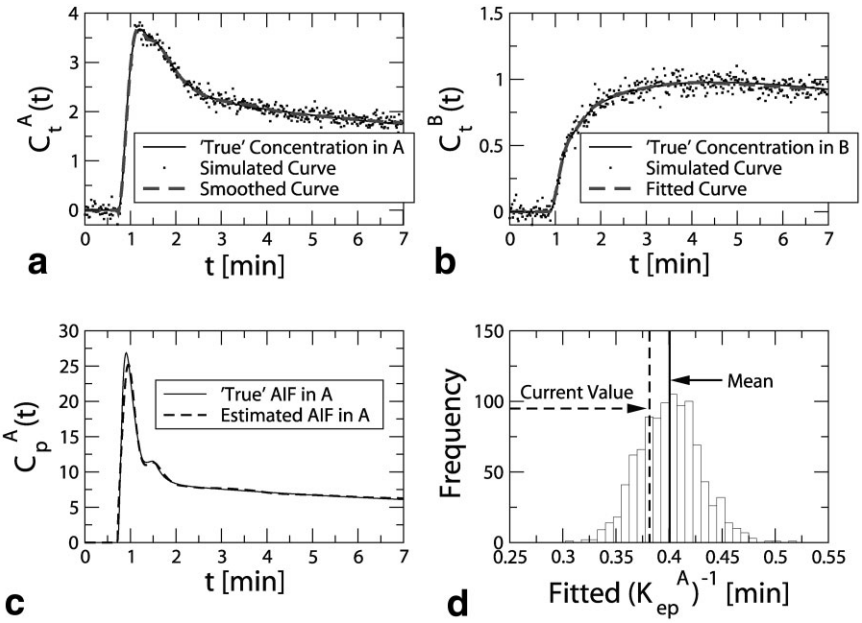

FIG. 2. Performance of the double-reference-tissue method illustrated by the simulated data set with median SSE out of the total of 1000 simulated ones created at $\beta^A = \beta^B = 0.02$ [min], noise level ($\sigma^A(t) = 0.10$, $\sigma^B(t) = 0.05$), and $l = 0.14$ [min]. **a:** The concentration-vs.-time curve in tissue A smoothed from the noisy simulated curve by local polynomial regression (dashed line) is a very good fit for the "true" curve used in the simulation (solid line). **b:** The concentration-vs.-time curve in tissue B fitted by the double-reference-tissue method (dashed line) is in good agreement with the "true" curve (solid line). **c:** For this data set with median performance, the AIF in tissue A estimated by the double-reference-tissue method (dashed line) is very close to the "true" AIF. **d:** The histogram of the total of 1000 fitted $(K^A_{ep})^{-1}$ estimated from the 1000 simulated data sets, the dashed line shows the fitted $(K^A_{ep})^{-1}$ of the current data set, which is the 26% quantile. The "true" value of $(K^A_{ep})^{-1}$ is 0.40.

and the "true" value. Figure 2a demonstrates the performance of local polynomial regression in smoothing the noisy concentration-vs.-time curve of tissue A, showing that the smoothed curve is a close match to the "true" curve. Figure 2b shows that we can achieve an excellent fit of the concentration-vs.-time curve in tissue B when the AIFs of the two tissues are the same. For the reconstruction of the AIF, we assume that the literature value of v_e^A is equal to the "true" value (that is, the value of 0.28 selected for the simulations). Figure 2c shows that the reconstructed AIF in tissue A closely resembles the "true" one, and even reproduces the second pass of the bolus correctly. Compared to the "true" AIF in tissue A, the first-pass part of this estimated AIF is somewhat distorted, with a slightly wider but lower peak. Part of the distortion is caused by bias in the smoothing of $\tilde{C}_t^A(t)$. With higher time resolution and SNR, the overlap between the estimated AIF and the true one would improve.

When the AIFs of the two reference tissues have different shapes due to the effects of different dispersions, the simulations show that the fitted parameters are biased. Figure 3 shows that when $\beta^A \neq \beta^B$, and hence the transport functions of the two reference tissues have different spread, the mean of the fitted $(K^A_{ep})^{-1}$ is not equal to its "true" value. Figure 3 shows that as the difference between β^A and β^B increases, the bias in the mean of fitted $(K^A_{ep})^{-1}$ increases, and when the difference is 0.03 min, the bias is only about 10%. At the noise level ($\sigma^A(t) = 0.10$, $\sigma^B(t) = 0.05$) that corresponds to an approximate SNR of 20, the half-width of the 95% C.I. of fitted $(K^A_{ep})^{-1}$ remains about 15% of the "true" value at different combinations of β^A and β^B; and it is halved when the noise level is reduced by half.

Given the effect of β^A and β^B in simulations, it is useful to estimate their orders to determine the degree of bias in real clinical data. In clinical applications of the double-reference-tissue method, we would choose two reference tissues in close anatomical proximity, such that the mean transit time (MTT) of the AIF from a common major artery to the reference tissues is several seconds or, at most, a few tens of seconds. In other words, the MTT is approximately 0.1–0.6 min. Many studies have shown that the SD of the transport function is about 0.2 times the MTT (19,27), i.e., the longer the transit time, the greater the dispersion. The

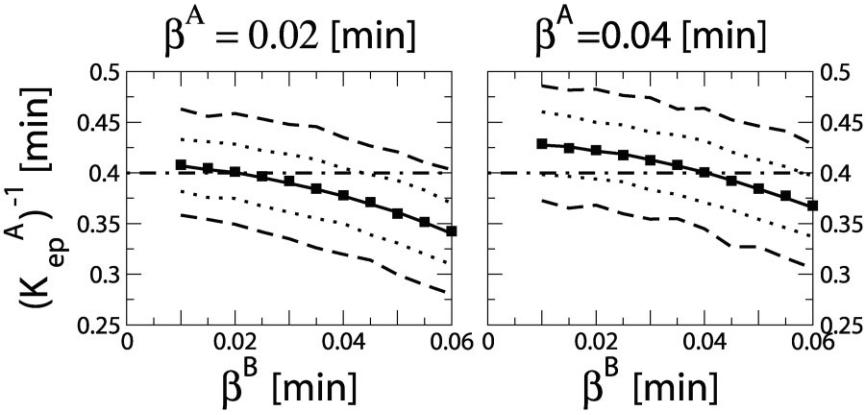

FIG. 3. Statistics of the fitted $(K^A_{ep})^{-1}$ with different combinations of β^A and β^B. We selected $l = 0.0$ [min] in the simulations shown here. Solid lines and dashed lines are respectively the mean and 95% C.I. of the fitted $(K^A_{ep})^{-1}$ at the noise level ($\sigma^A(t) = 0.10$, $\sigma^B(t) = 0.05$). Squares and dotted lines are respectively the mean and 95% C.I. of the fitted $(K^A_{ep})^{-1}$ at the noise level ($\sigma^A(t) = 0.05$, $\sigma^B(t) = 0.025$). The dot dashed lines show the "true" value of $(K^A_{ep})^{-1}$, which is 0.40 [min]. The mean of the fitted $(K^A_{ep})^{-1}$ is not equal to its "true" value when $\beta^A \neq \beta^B$.

SD of the transport function used in our simulation is equal to 2β, and therefore 2β ~ 0.2 MTT. This leads to an estimation of β^A and β^B between 0.01 and 0.06 min, according to the order of MTT mentioned above. This range of β^A and β^B is what we used in our simulations (Fig. 3). Given the range of β^A and β^B expected in clinical data, the difference between β^A and β^B is unlikely to exceed 0.03 min. This follows once again from the 2β ~ 0.2 MTT relationship, which reveals that a 0.03-min difference between β^A and β^B is equivalent to a difference of about 0.3 min between the MTT of the two reference tissues. A 0.3-min (nearly 20 s) difference in MTT is unlikely when the two reference tissues are chosen to be in close anatomical proximity. Importantly, and as described in the previous paragraph, a 0.03-min difference between β^A and β^B will result in about 10% systematic errors. Thus, our simulations suggest that the systematic errors due to dispersion effects are very likely <10% in clinical applications of the double-reference-tissue method.

DISCUSSION AND CONCLUSIONS

In this work we have presented a novel method to estimate the AIF from the contrast agent concentration-time curves of two reference tissues measured by DCE-MRI. Under the assumption that the AIFs of the two reference tissues have the same shape, the double-reference-tissue method at first establishes a connection between the two concentration-vs.-time curves so as to fit the kinetic parameters of the two reference tissues. Then the AIF is estimated with the fitted kinetic parameters by means of the reference-tissue approach. We used Monte Carlo simulations to evaluate the performance of the method, which showed that it gives an excellent estimate of the AIF for simulated data, with an SNR comparable to that of real clinical data. The simulations also estimated the magnitude of errors due to noise, as well as the discrepancy between the AIFs of the two tissues caused by their different dispersions. These simulations suggest that the random and systematic errors are small, and that the double-reference-tissue method will be reliable in clinical applications.

The simulations also show that differences in β^A and β^B will lead to bias in the estimates of kinetic parameters. As a further refinement of the double-reference-tissue method, one could estimate and even possibly reduce this bias by using experimental data to estimate the relative values of β^A and β^B. This could be done using the relationship between bolus arrival time and MTT, as discussed above. In addition, because β^A and β^B indicate the effect of dispersion in the two reference tissues, their amplitude is reflected by the width of the first-pass bolus. In truly high-time-resolution and high-SNR data, an excellent estimate of $dC_t(t)/dt$ can be obtained for each reference tissue. This can then be used to find the beginning and end of the first-pass bolus. The resultant width of the first-pass bolus of the two tissues can then be used to estimate the order of magnitude of β^A and β^B. Estimates of the difference between β^A and β^B could be used as evidence to neglect the bias if the differences are small, or as information to correct for the bias if the differences are large.

In the application of the double-reference-tissue method, we use data from a homogenous ROI of the normal reference tissues to increase the SNR. Sometimes it may be difficult to choose a continuous ROI whose pixels all have homogenous kinetic parameters—for example, in cases in which normal liver and muscle tissue have fatty infiltrations. In such cases, we use an iterative fitting procedure to eliminate pixels whose kinetic parameters differ significantly from those of other pixels. As the first step, we obtain an estimate of the AIF by using the mean concentration-vs.-time curves of all the pixels in the ROI. Second, we use the obtained AIF to fit the kinetic parameters for every pixel in the ROI. The pixels whose fitted kinetic parameters differ significantly are then eliminated. Finally, using the mean concentration-vs.-time curves of the remaining pixels, one can calculate an updated, more accurate estimate of the AIF. If the second step is repeated several times, the final remaining pixels in the ROI will be homogenous, and the final obtained AIF will be more precise.

In the simulations, we utilized a two-compartment model to determine kinetic parameters in the reference tissues. In animal models, the two-compartment model works well for normal tissues, particularly normal tissues with high blood flow (11). The two-compartment model also has relatively few adjustable parameters, and this is preferable for data with modest SNR. Although more complicated models (e.g., three-compartment models) may provide better fits to experimental data, the introduction of additional parameters will lead to greater errors in the parameter estimates, and a greater risk for degeneracy between kinetic parameters in the fitting algorithm. Although the double-reference-tissue method is applicable to any kinetic model, including models that take into account the intravascular contribution to the measured concentration, it remains preferable in practice to use the two-compartment model for normal tissues when it can provide an adequate fit to the data.

It is also preferable to use tissue with high blood flow and capillary permeability (such as liver or spleen) as one of the reference tissues, for three reasons: First, a two-compartment model is likely to be a good approximation for highly perfused tissues, so that the AIF in can be described by the simple expression in Eq. [7]. Second, since the concentration-vs.-time curve for rapidly perfused tissues has a higher SNR in the initial steep uptake period, the comparative errors in the nonparametric estimates of $C_t^A(t)$ and $dC_t^A(t)/dt$ are smaller. Third, because contrast media exchanges rapidly between blood and tissue, the contrast media concentration in the blood plasma is nearly in equilibrium with the concentration in the EES after the first few passes of the contrast bolus. This allows accurate measurement of the AIF during washout. It should be noted that the kidney's role in filtering and excreting low-molecular-weight contrast agents makes the use of this organ as a reference tissue problematic despite its high blood flow and capillary permeability.

The present demonstration of the double-reference-tissue method is based entirely on simulations. The simulations did not account for blood plasma's contribution to the measured contrast media concentration, or other, more complicated underlying pathophysiology (such as the liver's unique circulation system). The transport function of liver may be very different from the transport function

used in our simulations. In the liver, the contrast agent reaches the organ through the hepatic artery, which is a branch of the aorta, as well the hepatic portal vein, which transports venous blood from the splanchnic organs. Thus the current simulations may not correctly estimate the bias when liver is used as reference tissue A. Further clinical investigation should be considered to determine whether the liver is a good reference tissue for the double-reference-tissue method.

Given the promising results suggested by the simulations here, the next step will be to test the performance of the method in practice. The parameters obtained with the present method must be compared with the AIF and/or kinetic parameters estimated with other methods and/or with contrast media concentration measured in blood samples. If such studies confirm that the double-reference-tissue method is accurate, it could then be used to derive the AIF for more complicated tissues, such as tumor tissue. This would allow more accurate estimations of the kinetic parameters, which in turn have been proposed as useful pharmacodynamic and predictive markers for vascular-targeted therapy.

REFERENCES

1. Kety SS. Regional cerebral blood flow: estimation by means of nonmetabolized diffusible tracers—an overview. Semin Nucl Med 1985;15:324–328.
2. Tofts PS, Kermode AG. Measurement of the blood-brain barrier permeability and leakage space using dynamic MR imaging. I. Fundamental concepts. Magn Reson Med 1991;17:357–367.
3. Tofts PS, Brix G, Buckley DL, Evelhoch JL, Henderson E, Knopp MV, Larsson HB, Lee TY, Mayr NA, Parker GJ, Port RE, Taylor J, Weisskoff RM. Estimating kinetic parameters from dynamic contrast-enhanced T(1)-weighted MRI of a diffusable tracer: standardized quantities and symbols. J Magn Reson Imaging 1999;10:223–232.
4. Padhani AR, Husband JE. Dynamic contrast-enhanced MRI studies in oncology with an emphasis on quantification, validation and human studies. Clin Radiol 2001;56:607–620.
5. Parker GJ, Tanner SF, Leach MO. Pitfalls in the measurement of tissue permeability over short-scales using a low temporal resolution blood input function. In: Proceedings of the 4th Annual Meeting of ISMRM, New York, 1996. p 1582.
6. Port RE, Knopp MV, Hoffmann U, Milker-Zabel S, Brix G. Multicompartment analysis of gadolinium chelate kinetics: blood–tissue exchange in mammary tumors as monitored by dynamic MR imaging. J Magn Reson Imaging 1999;10:233–241.
7. Fritz-Hansen T, Rostrup E, Larsson HB, Sondergaard L, Ring P, Henriksen O. Measurement of the arterial concentration of Gd-DTPA using MRI: a step toward quantitative perfusion imaging. Magn Reson Med 1996;36:225–231.
8. Calamante F, Gadian DG, Connelly A. Delay and dispersion effects in dynamic susceptibility contrast MRI: simulations using singular value decomposition. Magn Reson Med 2000;44:466–473.
9. Hoffmann U, Brix G, Knopp MV, Hess T, Lorenz WJ. Pharmacokinetic mapping of the breast: a new method for dynamic MR mammography. Magn Reson Med 1995;33:506–514.
10. St Lawrence KS, Lee TY. An adiabatic approximation to the tissue homogeneity model for water exchange in the brain: II. Experimental validation. J Cereb Blood Flow Metab 1998;18:1378–1385.
11. Kovar DA, Lewis M, Karczmar GS. A new method for imaging perfusion and contrast extraction fraction: input functions derived from reference tissues. J Magn Reson Imaging 1998;8:1126–1134.
12. Rippe C, Rippe B, Erlanson-Albertsson C. Capillary diffusion capacity and tissue distribution of pancreatic procolipase in rat. Am J Physiol 1998;275(5 Pt 1):G1179–G1184.
13. Fan J, Gijbels I. Local polynomial modelling and its applications. New York: Chapman & Hall; 1996.
14. Eubank RL. Nonparametric regression and spline smoothing. New York: Marcel Dekker, Inc.; 1999.
15. Ostergaard L, Weisskoff RM, Chesler DA, Gyldensted C, Rosen BR. High resolution measurement of cerebral blood flow using intravascular tracer bolus passages. Part I: Mathematical approach and statistical analysis. Magn Reson Med 1996;36:715–725.
16. Evans RL. Two comments on the estimation of blood flow and central volume from dye-dilution curves. J Appl Physiol 1959;14:457.
17. Thompson Jr HK, Starmer CF, Whalen RE, McIntosh HD. Indicator transit time considered as a Gamma variate. Circ Res 1964;14:502–515.
18. Stow RW, Hetzel PS. An empirical formula for indicator-dilution curves as obtained in human beings. J Appl Physiol 1954;7:161–167.
19. Bassingthwaighte JB, Ackerman FH, Wood EH. Applications of the lagged normal density curve as a model for arterial dilution curves. Circ Res 1966;18:398–415.
20. Bassingthwaighte JB. Physiology and theory of tracer washout techniques for the estimation of myocardial blood flow: flow estimation from tracer washout. Prog Cardiovasc Dis 1977;20:165–189.
21. Andersen C, Taagehoj JF, Muhler A, Rehling M. Approximation of arterial input curve data in MRI estimation of cerebral blood-tumor-barrier leakage: comparison between Gd-DTPA and 99mTc-DTPA input curves. Magn Reson Imaging 1996;14:235–241.
22. Li KL, Zhu XP, Waterton J, Jackson A. Improved 3D quantitative mapping of blood volume and endothelial permeability in brain tumors. J Magn Reson Imaging 2000;12:347–357.
23. Padhani AR, Hayes C, Landau S, Leach MO. Reproducibility of quantitative dynamic MRI of normal human tissues. NMR Biomed 2002;15:143–153.
24. van Laarhoven HW, Rijpkema M, Punt CJ, Ruers TJ, Hendriks JC, Barentsz JO, Heerschap A. Method for quantitation of dynamic MRI contrast agent uptake in colorectal liver metastases. J Magn Reson Imaging 2003;18:315–320.
25. Press WH, Teukolsky SA, Vetterling WT, Flannery BP. Numerical recipes in C. New York: Cambridge University Press; 1992.
26. Medved M, Karczmar G, Yang C, Dignam J, Gajewski TF, Kindler H, Vokes E, MacEneany P, Mitchell MT, Stadler WM. Semi-quantitative analysis of dynamic contrast enhanced MRI in cancer patients: variability and changes in tumor tissue over time. J Magn Reson Imaging 20:122–128.
27. King RB, Deussen A, Raymond GM, Bassingthwaighte JB. A vascular transport operator. Am J Physiol 1993;265(6 Pt 2):H2196–H2208.